

# Liposome entrapment and immunogenic studies of a synthetic lipophilic multiple antigenic peptide bearing VP1 and VP3 domains of the hepatitis A virus: a robust method for vaccine design

Isabel Haro<sup>a,\*</sup>, Silvia Pérez<sup>a</sup>, Mónica García<sup>a</sup>, Weng C. Chan<sup>b</sup>, Guadalupe Ercilla<sup>c</sup>

<sup>a</sup>Departament de Química de Pèptids i Proteïnes, IIQAB-CSIC, Jordi Girona 18–26, 08034 Barcelona, Spain

<sup>b</sup>School of Pharmaceutical Sciences, University of Nottingham, University Park, Nottingham NG7 2RD, UK

<sup>c</sup>Servei d'Immunologia, IDIBAPS, Hospital Clinic i Provincial, Barcelona, Spain

Received 9 December 2002; accepted 25 February 2003

First published online 14 March 2003

Edited by Hans-Dieter Klenk

**Abstract** Multiple antigen peptides (MAP) have been demonstrated to be efficient immunological reagents for the induction of immune responses to a variety of infectious agents. Several peptide domains of the hepatitis A virus (HAV) capsid proteins, mainly VP1 and VP3, are the immunodominant targets for a protective antibody response. In the present study we analyse the immunogenic properties of a tetrameric heterogeneous palmitoyl-derivatised MAP containing two defined HAV peptide sequences, VP1(11–25) and VP3(102–121), in rabbits immunised with either Freund's adjuvant or multilamellar liposomes. The immune response was evaluated with a specific enzyme immunoassay using MAP[VP1+VP3], VP1 and VP3 as targets. The avidity of the immune response was measured by a non-competitive enzyme-linked immunosorbent assay and by the surface plasmon resonance technology. Antisera raised against the lipo-MAP peptide entrapped in liposomes demonstrated high avidity of binding with affinity rate constants approximately one order of magnitude greater than those obtained with the Freund's protocol.

© 2003 Federation of European Biochemical Societies. Published by Elsevier Science B.V. All rights reserved.

**Key words:** Hepatitis A virus; Multiple antigenic peptide; Peptide synthesis; Liposome; Enzyme-linked immunosorbent assay; Surface plasmon resonance

## 1. Introduction

The practical development of modern vaccines has been greatly advanced by the availability of synthetic antigens. The use of such synthetic antigens might be more acceptable

for human therapy since synthetic peptides do not have any of the potential dangers associated with the induction of an infection by recombinant viruses. However, progress has been hindered in some cases by poor immunogenicity of the antigens. This handicap can be overcome by the use of potent immunoadjuvants, though only few adjuvants used in experimental models are allowed for use in man.

Multiple antigen peptides (MAP) [1], synthetic macromolecules containing defined B and/or T cell epitopes of one or more antigens, have been demonstrated to be efficient immunological reagents for the amplification in the analysis and induction of immune responses to a variety of infectious agents [2].

Recently, we reported the synthesis and the immunogenicity of several peptide sequences derived from hepatitis A virus (HAV) capsid proteins when administered to laboratory animals in different forms [3–5]. Overall, the VP3(102–121) peptide sequence appeared to be more immunogenic than VP1 and VP2 peptides. The highest anti-HAV titres were also observed in mice immunised with VP1 and, particularly, VP3 peptides and neutralisation of HAV infectivity was achieved. Moreover, immune responses generated by peptides entrapped in liposomes were of higher magnitude than those induced by free peptides.

Besides, in a previous work we have reported investigative results about the antigenicity of a diepitope MAP containing the sequences HAV-VP1(11–25) and HAV-VP3(110–121). Our results have shown that branched peptides could be very useful for the development of new diagnostic tests [6–8].

Modification of the lipophilic properties of peptides has been used in the development of an immunisation strategy. It has been reported that the use of a covalently coupled fatty acid moiety enhances the immunogenicity of an unmodified peptide [9]. A hypothesis has been proposed on the affinity of lipid chains for cell membranes, targeting the peptide to the cell surface followed by passive diffusion across the cell membrane, delivery to the cytosol and migration into the cell compartments [10,11]. The conventional design of MAP without a lipophilic adjuvant attachment has been successful in many systems to elicit high-titre antibodies in animals [12–14]. However, the advantages of a MAP with a built-in adjuvant are quite clear. It removes the obstacle of an extraneous adjuvant and it can be used in a macromolecular assemblage approach containing a combination of needed peptide antigens, a non-immunogenic core matrix as a carrier, a built-in palmitoyl

\*Corresponding author. Fax: (34)-93-2045904.  
E-mail address: [ihvqpp@iiqab.csic.es](mailto:ihvqpp@iiqab.csic.es) (I. Haro).

**Abbreviations:** Boc, *tert*-butoxycarbonyl; DIEA, *N,N*-diisopropylethylamine; DIPCDI, *N,N*-diisopropylcarbodiimide; DMF, dimethylformamide; ELISA, enzyme-linked immunosorbent assay; Fmoc, fluorenylmethoxycarbonyl; HAV, hepatitis A virus; HOBt, *N*-hydroxybenzotriazole; HPLC, high-performance liquid chromatography; MAP, multiple antigenic peptides; MLV, multilamellar vesicles; MS, mass spectrometry; OD, optical density; RU, resonance units; SPR, surface plasmon resonance; TBTU, 2(1*H*-benzotriazol-1-yl)-1,1,3,3-tetramethyluronium tetrafluoroborate; TFA, trifluoroacetic acid; TIPS, triisopropylsilane

moiety as the adjuvant and liposomes as the vehicle. All these are required components for an effective vaccine formulation.

Taking into account our previous results and since the combination of adjuvant effects of liposomes and a built-in lipid anchor could replace the need for an extraneous adjuvant such as Freund's, which is toxic and unacceptable in humans, we herein report the design, synthesis and immunogenic studies of a tetrameric heterogeneous MAP containing two of the HAV peptide sequences previously described, specifically VP1(11–25) and VP3(101–121), as well as the lipid tail of palmitic acid.

## 2. Materials and methods

### 2.1. Peptide synthesis

The synthesis of the diepitopic lipophilic MAP shown in Fig. 1 was carried out in a 0.1 mmol scale utilising a continuous flow fluoren-9-ylmethoxycarbonyl (Fmoc) method [15]. A NovaSyn™ TG resin (polyethylene glycol-linked PS) functionalised with Rink amide linker (0.2 mmol/g) was used in a continuous flow Milligen 9050 PepSynthesizer™. The general strategy that was followed for the synthesis of the MAP construct is summarised in Fig. 2.

Following removal of the linker Fmoc-protecting group, by continuous flow (3.50 ml/min) treatment with 20% piperidine–dimethylformamide (DMF) for 6 min, 0.3 mmol of Dde-Lys(Fmoc)-OH [16] previously activated with 2-(1*H*-benzotriazol-1-yl)-1,1,3,3-tetramethyluronium tetrafluoroborate:*N*-hydroxybenzotriazole:*N,N*-diisopropylethylamine (TBTU:HOBt:DIEA, 1:1:2) was coupled to the linker. The coupling was complete in 2 h as judged by the picrylsulphonic acid test [15].

*N*<sup>ε</sup>-Acylation with palmitic acid was carried out by, firstly, removal of the *N*<sup>ε</sup>-Fmoc-protecting group followed by addition of a triple excess of palmitic acid that was activated with *N,N*-diisopropylcarbodiimide (DIPCDI) and HOBt (1:1). The reaction mixture was gently agitated overnight and checked by the picrylsulphonic acid test for completion of the reaction.

The *N*<sup>ε</sup>-Dde-protecting group was then removed by treatment with 2% hydrazine in DMF [16]. Deprotection was monitored by the absorption of the resulting 3,6-trimethyl-4-oxo-4,5,6,7-tetrahydro-1*H*-indazole at 300 nm and was completed within 10 min.

The tetravalent lysine core was obtained by sequential coupling of 0.4 mmol of Fmoc-Lys(Fmoc)-OH and 0.8 mmol of Fmoc-Lys(Dde)-OH, which were incorporated through TBTU:HOBt:DIEA (1:1:2)-mediated carboxyl activation.

The assembly of the peptide sequence HAV-VP1(11–25) was then accomplished at both *N*<sup>α</sup>-lysine positions. Amino acid side chain protection was effected by the following: trityl (triphenylmethyl) for glutamine and asparagine; *tert*-butyl for aspartic acid, glutamic acid, serine and threonine. An eightfold molar excess of Fmoc-amino acids, TBTU, HOBt and DIEA (1:1:1:2) was used throughout the synthesis

in a stepwise manner. The reaction column effluent was subjected to continuous UV monitoring by passage through an Ultrospec II LKB 4050™ spectrophotometer at 290 nm. Typical acylation and deprotection traces were obtained indicating satisfactory progress in assembly. Double coupling was used to introduce the asparagine residue. The peptide assembly was terminated by *N*-capping with di-*tert*-butyl dicarbonate.

At this point, the lysine core *N*<sup>ε</sup>-Dde group was deprotected by treatment with 2% hydrazine in DMF. A small amount of the peptidyl resin was removed from the reaction column, washed with DMF, dichloromethane and methanol, and dried in vacuo. The monoepitopic lipophilic MAP was concomitantly side chain-deprotected and cleaved from the resin by treatment with a mixture of TFA in the presence of triisopropylsilane (TIPS) and water as scavengers (TFA:TIPS:H<sub>2</sub>O, 9.5:0.25:0.25) for 6 h with occasional agitation at room temperature. Then, the resin was filtered and washed with TFA. The filtrate was evaporated in vacuo to dryness and the crude peptide was precipitated with diethyl ether (10 ml) to afford a white solid, which was collected, dissolved in water (25 ml) and lyophilised.

Reversed-phase high-performance liquid chromatography (HPLC) analysis was performed on a Hypersil 300 Å C18 column (4.6 × 150 mm). The eluents were A: H<sub>2</sub>O (0.05% TFA) and B: 90% MeCN:10% H<sub>2</sub>O (0.05% TFA). The elution profile was a linear gradient of 5–100% B in 40 min at a flow rate of 1.20 ml/min, and a major elution peak with a retention time of 26 min was observed.

Electrospray mass spectrometry (MS) spectra confirmed the expected molecular mass of the lipophilic monoepitopic MAP ([MH<sup>+</sup>] = 3900.2). Purification of the crude molecule was achieved by preparative HPLC on a Kromasil C-8 column. The flow rate was 4.5 ml/min with a gradient of 40–70% B in 20 min.

The assembly of the HAV-VP3(101–121) sequence was then performed at both exposed lysine *N*<sup>ε</sup>-amino groups of the monoepitopic lipophilic MAP resin intermediate. During the synthesis of the VP3 sequence, the Cys residues present in the native peptide were replaced by 2-aminobutyric acid (Abu) residues. This amino acid has the same hydrophobic and steric properties as cysteine, but avoids the reactivity of the Cys thiol group without modifying the immunochemical properties of the parent peptide [17]. During peptide assembly, trifunctional amino acids were side chain-protected by the following: 2,2,5,7,8-pentamethyl-chroman-6-sulphonyl for arginine; trityl for glutamine; *tert*-butyl for aspartic acid and serine; and *tert*-butoxycarbonyl (Boc) for tryptophan.

The two initial amino acid residues of the sequence were coupled manually and double coupling was used for the remainder in order to ensure efficiency of the synthesis.

The final protected diepitopic peptidyl resin was collected as before, dried in vacuo, and treated with the following cleavage mixture: TFA:H<sub>2</sub>O:1,2-ethanedithiol:TIPS (9.25:0.25:0.25:0.25) at 25°C for 6 h. The reaction mixture was filtered, the filtrate was evaporated to dryness in vacuo and the residual peptide material was precipitated with diethyl ether to give a white solid. The crude peptide was then suspended in water (25 ml) and lyophilised. Electrospray MS analysis showed the presence of the expected diepitopic lipophilic MAP ([MH<sup>+</sup>] = 8846.55) after partial purification by ultracentrifugation in water. The semi-purified MAP synthetic construct was also characterised by amino acid analysis as shown in Table 1.

### 2.2. Peptide entrapment in liposomes

Multilamellar vesicles (MLV liposomes) were prepared as previously described [3]. Briefly, 40 mg of phosphatidylcholine, 20 mg cholesterol and 3 mg of lipophilic MAP were evaporated from a chloroform–methanol (2:1, v/v) solution. The samples were subjected to the vacuum of an oil pump to eliminate the last traces of the solvents. A 0.9% aqueous NaCl solution was added to the dry lipid peptide, and the suspension gently stirred for 1 h at room temperature. After preparation, the MLV liposomes were washed two times by successive centrifugation at 25000 × *g* and resuspension of the pellets in 0.9% saline. The peptide content of liposomes was determined by quantitative amino acid analysis. The analysis was carried out in a Pico-Tag™ system (Waters, Stockport, UK). Sample was hydrolysed in 6 M HCl at 110°C for 24 h. Vesicle size was determined by measurement of the sample diffusion coefficient using photon correlation spectroscopy. The phospholipid content was determined as previously described [18], and the characterisation of the liposomes–MAP-[VP1+VP3] preparation is summarised in Table 2.

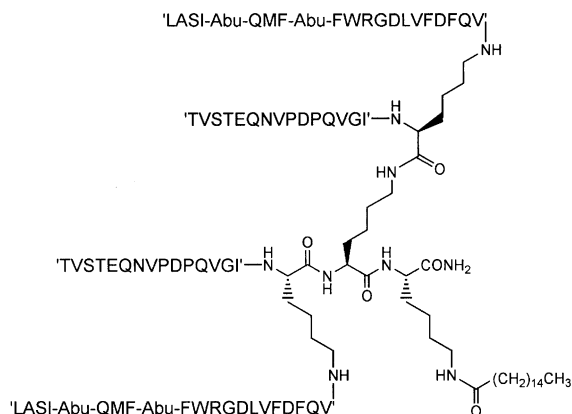


Fig. 1. Primary structure of MAP[VP1+VP3].

### 2.3. Antibody production

Anti-peptide sera were prepared by immunising two rabbits with the free peptide and the liposome-entrapped peptide following the inoculation protocol outlined below.

One animal (rabbit 1) was immunised subcutaneously with 200  $\mu\text{g}$  in 1 ml of heterogeneous MAP[VP1+VP3] with an equal volume of complete Freund's adjuvant (Difco, Detroit, MI, USA). The second animal (rabbit 2) was immunised with the same peptide, MAP[VP1+VP3] anchored on liposomes without adjuvant. Animals were boosted with four injections of 200  $\mu\text{g}$  of peptides either in combination with incomplete Freund's adjuvant or in MLV liposomes at 3-week intervals.

Serum samples were obtained before each immunisation and also 1 week after inoculation. Animal care procedures complied with the Institutional Animal Care and Use Committee Guidelines.

Polyclonal IgG were purified by protein G affinity (HiTrap<sup>®</sup> protein G, Pharmacia Biotech) according to standard procedures. One millilitre on rabbit antiserum was adsorbed to the column in binding buffer (20 mM sodium phosphate, pH 7.0); after washing, bound IgG was eluted with 0.1 M citric acid, pH 3.5. The collected fractions were immediately neutralised to pH 7.2 with 1 M Tris-HCl pH 9.0. Immunoglobulin concentrations were established by spectrophotometry. The fractions with the highest absorbance were pooled to afford 600  $\mu\text{g}/\text{ml}$  final concentrations.

### 2.4. Enzyme-linked immunosorbent assay (ELISA)

In order to characterise the immune reactivity of sera towards the MAP[VP1+VP3], VP1 and VP3 peptide sequences, the synthetic peptides were used as coating agents in ELISA microplates.

The synthetic peptides were diluted with coating buffer (0.2 M carbonate/bicarbonate-buffered saline, pH 9.7) to a final concentration of 10  $\mu\text{g}/\text{ml}$  and 100  $\mu\text{l}$  was added to each microwell (Maxisorp, 96F, Nunc, Roskilde, Denmark). The microtitre plates were incubated at room temperature overnight. After washing the plates with phosphate-buffered saline (PBS), pH 7.2, containing 0.05% Tween 20, unoccupied binding sites were blocked with 300  $\mu\text{l}$  of PBS containing 3% skimmed milk powder at room temperature for an additional 2 h. Then, the plates were rinsed with washing buffer, dried and frozen for later use in the detection of antibodies against MAP[VP1+VP3], VP1 and VP3 peptides.

For non-competitive ELISA assays, on each peptide-coated microwell, 100  $\mu\text{l}$  of serum (diluted 1/100 with PBS containing 3% skimmed milk powder) was incubated at room temperature overnight. The microwells were washed three times with washing buffer before the addition of 100  $\mu\text{l}$  of horseradish peroxidase-conjugated goat anti-rabbit IgGs as detector antibodies (Dakopatts, Dako, Denmark), and were incubated for 2 h at room temperature. After washing the microwells three times, the colour was developed by adding 100  $\mu\text{l}$  of the substrate (4  $\mu\text{l}$   $\text{H}_2\text{O}_2$  in 50 mM sodium phosphate-citric acid buffer, pH 5.0, containing 0.4 mg/ml *o*-phenylenediamine dihydrochloride (Sigma)).

### 2.5. Avidity calculation

A protocol based on Beatty's calculations was used to measure affinity in monoclonal antibodies [19]. This method is based on the law of mass action and uses the total antibody concentration added per well rather than the bound or free ratio. The method does not require affinity purification of the standard specific antibody used by other methods [20].

Microplates were sensitised, in the same conditions as described above, with different MAP[VP1+VP3] concentrations (0.125, 0.062, 0.031 and 0.015  $\mu\text{g}/\text{ml}$ ). Each peptide concentration was incubated with 1/4 serial dilutions of the purified IgG corresponding to each serum sample for 1 h at room temperature. After washing, the microplates were incubated with 1/1000 horseradish peroxidase-conjugated goat  $\gamma$ -chain-specific anti-rabbit (Dakopatts). The assay was then developed as described above for the non-competitive ELISA.

The ELISA curves of optical density (OD) at 492 nm versus the logarithm of concentration were sigmoid in nature. The method is based upon the law of mass action and uses the total antibody concentration added per well [Ab]. The method compares the OD-50 of two sigmoid curves of antibody serial dilutions on plates coated with two different antigen concentrations. The OD at any point of the sigmoid dilution curve of OD versus the logarithm of concentration is presumed to be a direct reflection of the amount of antibody bound

to the antigen in the well. At 50% of OD-100, OD-50, the amount of antibody bound to antigen in the well is half the amount of antibody bound at OD-100. Taking into account the combination of antigen concentration in the well and the dilution of the sera, an estimation of the constant of affinity ( $K_a$ ) can be formulated as:  $K_a = 1/2 (2[\text{Ab}_t \text{ at OD-50}] \text{ minus } [\text{Ab}_t \text{ at OD-100}])$ .

### 2.6. Surface plasmon resonance (SPR) studies

To evaluate the biospecific interactions between purified IgG antibodies raised against the MAP[VP1+VP3] peptide, we also used biosensor technology. The Biacore 1000 analytical instrument, sensor chip CM5 and maintenance kit, the amine coupling kit containing *N*-hydroxysuccinimide, *N*-ethyl-*N'*-(3-diethylaminopropyl)-carbodiimide, ethanolamine hydrochloride adjusted to pH 8.5 using NaOH and the running buffer (HBS) containing 10 mM HEPES pH 7.4, 150 mM NaCl, 3.4 mM EDTA and 0.005% surfactant P20 were provided by Biacore (Saint Quentin-en-Yvelines, France). CM dextran sodium salt and sodium acetate were obtained from Fluka. All buffers were filtered and thoroughly degassed prior to use.

Several parameters were studied to optimise the binding method. Different pH values and different peptide concentrations were assayed. Finally, immobilisation was performed at 25°C and at a flow rate of 10  $\mu\text{l}/\text{min}$  in HBS as a running buffer following the procedure previously described [8]. To generate the coupled peptide injections, dissociation buffer was used prior to the regeneration cycle (1 min pulse with 100 mM NaOH). The flow rate of the IgG samples was constant at 10  $\mu\text{l}/\text{min}$ . Control experiments were performed using sensor chips activated according to the protocol described but without peptide coupled.

Prior to using the IgG solutions, the diluent buffer (Tris-HCl, pH 9.0) was replaced by the HBS BIA buffer (100 mM HEPES pH 7.4, 150 mM NaCl, 3.4 mM EDTA and 0.005% v/v surfactant P20). Exchange was performed on a G-25 Sephadex column (NAP-5, Pharmacia Biotech). The IgG concentration range was quantified by spectrometry and used at 600  $\mu\text{g}/\text{ml}$ .

The resonance signal (absolute response in resonance units (RU)) was recorded continuously during passage of a sample and the difference between the optical signals measured before and after serum injection (relative response in RU) was related to the amount of bound antibodies anti-HAV peptides. The contact time between a sample and the specific surface was 10 min. Dissociation of bound antisera was observed for 10 min. The same peptide surface was used repeatedly to study all the samples. This was accomplished by washing away the associated antibodies by an injection of 10  $\mu\text{l}$  of 100 nM NaOH between tests. Sensor chips were stored between experiments at 4°C in a capped test tube containing running buffer.

Real-time binding interactions between the MAP[VP1+VP3] peptide linked to a biosensor matrix and antibodies free in solution were recorded as RU and are displayed with respect to the time (*x*-axis) along the *y*-axis of a sensorgram. The integrated BIAevaluation 3.1 software was employed to calculate kinetics.

Data points from the early part of the dissociation phase were fitted to the manufacturer's model equations for calculations of dissociation rate constant ( $K_d$ ,  $\text{s}^{-1}$ ) for each polyclonal antiserum. Comparison of the binding avidity of antibodies in different sera was performed by measurement of the reciprocal ( $1/K_d$ ) of the dissociation constants [21].

## 3. Results

Synthesis of the macromolecular construct MAP[VP1+VP3] was successfully accomplished using a combination of orthogonal Dde amino protection and Fmoc-based solid-phase chemistry [15,16]. The overall synthetic strategy for the unambiguous assembly of the diepitopic lipophilic MAP that is based on a tetrameric lysine core is summarised in Fig. 2. Analysis by MS was carried out during the synthesis, in which the monoepitopic MAP intermediate was cleaved from the polymer support and subjected to both reversed-phase HPLC and electrospray MS analysis. For the final macromolecular product, after cleavage from the polymer support, the identity of the purified synthetic protein construct was con-

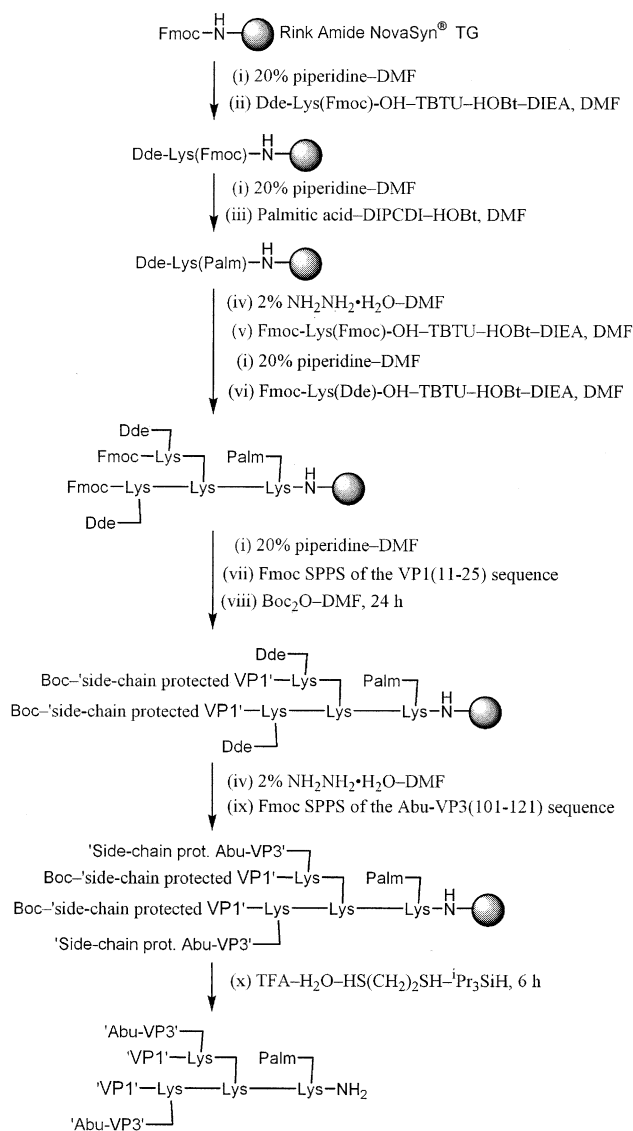


Fig. 2. Strategy of solid-phase peptide synthesis (SPPS) of MAP[VP1+VP3].

firmed by electrospray MS, and a satisfactory amino acid analysis (Table 1).

For formulation of an effective immunogenic preparation, MLV liposomes were selected in order to achieve good yields in the MAP[VP1+VP3] construct bears the lipid tail of the palmitoyl moiety, it was incorporated into the lipid mixture from the beginning of the process of liposome preparation, thus increasing the entrapment efficiency. The MAP[VP1+VP3] peptide/phospholipid ratio shown in Table 2 was high enough to carry out the inoculation protocol in a similar way as for the non-entrapped immunogen.

Both rabbits immunised with the synthetic MAP[VP1+VP3] peptide mounted a high antibody response. The antibody titre increased significantly after the second immunisation and reached a plateau after the third injection (Fig. 3A,B). Furthermore, antibody titres 1 month after the last immunisation were observed to decrease in rabbit 1. In contrast, the sera of rabbit 2 immunised using the liposome formulation continued to display strong antibody titres detectable at 1/100 dilution

Table 1  
MAP characterisation by amino acid analysis

Asx (Asp+Asn)	7.3 (8)
Thr	3.3 (4)
Ser	2.5 (4)
Glx (Glu+Gln)	9.3 (10)
Pro	4.1 (4)
Gly	4.2 (4)
Ala	2.0 (2)
Val	11.1 (10)
Met	0.4 (2)
Ile	4.1 (4)
Leu	3.6 (4)
Phe	7.7 (8)
Lys	4.5 (4)
Arg	1.7 (2)
Trp	n.d.

Theoretical values are in parentheses. Trp was not determined, and Ser, Thr and Met are known to undergo some degradation during 6 M HCl hydrolytic treatment.

up to 3 months (data not shown). Furthermore, the specificity of the response was confirmed by competitive ELISA: only the MAP peptide, up to nanomolar concentrations, was able to inhibit the enzyme immunoassay.

Immune sera recognised the inoculating peptide MAP[VP1+VP3] in both animals, but only animal 2 recognised independently both linear peptide components of MAP[VP1+VP3], these being the VP1(11–25) and VP3(102–121) peptide sequences, at high titres after the third immunisation. The animal immunised with Freund's adjuvant displayed a slight and transient response to VP1 peptide but no response to VP3 peptide (Fig. 3).

In order to analyse whether the immune responses mounted in rabbits were equivalent to those in humans we performed a competitive assay, as previously described [7], using an anti-human absorbed anti-IgG horseradish peroxidase not reacting with rabbit as second antibody. Rabbit antibodies were able to compete with the human antiserum, confirming that the synthetic peptide could mimic the B cell epitopes of native proteins (data not shown). We have previously described that the peptide formulations used in this study were recognised by the immune sera from patients suffering an acute hepatitis A infection [7].

To compare the affinity of antibodies induced by both immunisation protocols, we performed studies with both biosensor and enzyme immunoassay methods. Protein G affinity-purified IgG was obtained from each serum sample, and the test was standardised for the same concentration of 600 µg/ml. We decided not to use peptide affinity-purified antibodies in order to not discriminate antibodies with higher affinity displaying non-realistic results. We assume that following protein A affinity purification, differences in peptide binding could be attributed to differences in avidity of total IgG.

Using Beatty's approach, the  $K_a$  for rabbit 1, immunised

Table 2  
Vesicle size and peptide and phospholipid of MAP-liposome conjugate

Size (nm)	2370
Polydispersity	0.97
Phospholipid content (mg/ml)	7.7
Peptide content (mg/ml)	0.7
Peptide (mg)/phospholipid (mg)	0.09

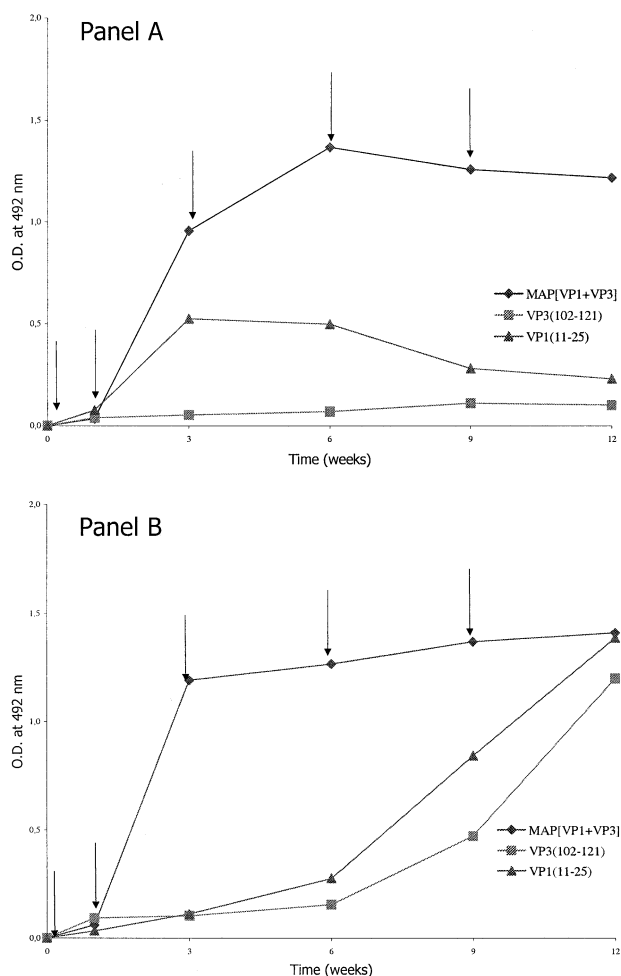


Fig. 3. Time course and IgG responses obtained in rabbits after immunisation with MAP[VP1+VP3]. Immunisations are indicated by the arrows and antibody specificity of bleedings is indicated as follows: rhombs MAP[VP1+VP3], triangles VP1 and squares VP3 in rabbits immunised with complete Freund's adjuvant (A) and MLV (B).

with Freund's adjuvant protocol, ranged between  $2.88$  and  $7.30 \times 10^6 \text{ M}^{-1}$ . The calculated  $K_a$  for rabbit 2, immunised with MAP entrapped liposomes, was  $4.56 \times 10^6$  to  $2.90 \times 10^7 \text{ M}^{-1}$  (Table 3). Furthermore, the sera from this animal dis-

Table 3  
Kinetic analysis of purified IgG with MAP[VP1+VP3] using SPR and ELISA

Weeks	SPR			ELISA			
	400 µg/ml			200 µg/ml			$K_a \text{ (M}^{-1}\text{)}$
	RU	$K_d \text{ (s}^{-1}\text{)}$	$1/K_d \text{ (s)}$	RU	$K_d \text{ (s}^{-1}\text{)}$	$1/K_d \text{ (s)}$	
Rabbit 1							
3	920	$5.81 \times 10^{-4}$	1 720	580	$5.26 \times 10^{-4}$	1 900	$2.88 \pm 1.23 \times 10^6$
6	295	$5.07 \times 10^{-4}$	1 970	180	$4.31 \times 10^{-4}$	2 320	$7.30 \pm 0.33 \times 10^6$
9	250	$4.58 \times 10^{-4}$	2 180	200	$4.03 \times 10^{-4}$	2 480	$7.05 \pm 0.43 \times 10^6$
12	220	$4.95 \times 10^{-4}$	2 020	105	$4.95 \times 10^{-4}$	2 020	$4.01 \pm 0.78 \times 10^6$
Rabbit 2							
3	695	$6.28 \times 10^{-4}$	1 590	470	$6.65 \times 10^{-4}$	1 500	$4.56 \pm 0.75 \times 10^6$
6	382	$2.38 \times 10^{-4}$	4 200	215	$2.22 \times 10^{-4}$	4 500	$4.76 \pm 1.85 \times 10^6$
9	350	$7.06 \times 10^{-5}$	14 200	260	$1.98 \times 10^{-4}$	5 050	$5.11 \pm 1.89 \times 10^6$
12	702	$3.81 \times 10^{-6}$	262 000	480	–	–	$2.90 \pm 0.68 \times 10^7$

Rabbit 1 was immunised with Freund's adjuvant and rabbit 2 with a liposome formulation. The dissociation rate constants ( $K_d$ ) from SPR were obtained from the resulting sensorgrams of two different IgG concentrations, 400 µg/ml and 200 µg/ml. The reciprocal dissociation rate constant ( $1/K_d$ ) was also calculated. ELISA results show the avidity constant obtained by means of equations based on the law of mass action.

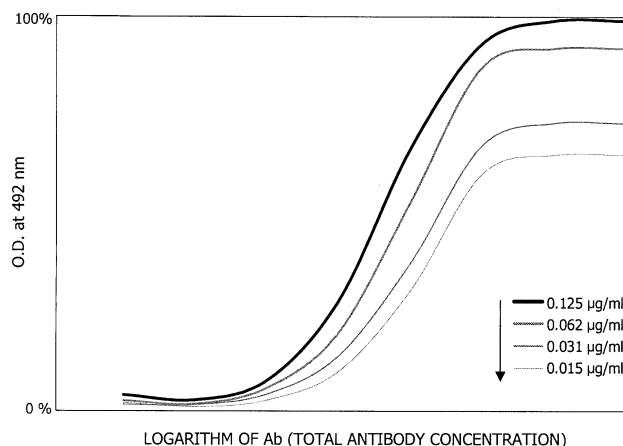


Fig. 4. Experimental enzyme immunoassay curve for purified IgG at different MAP[VP1+VP3] coating concentrations. The concentrations of MAP[VP1+VP3] in the coating solution were: 0.125, 0.063, 0.031 and 0.015 µg/ml. The calculated antibody concentrations at OD-50 were respectively: 3.276, 4.992, 8.580 and 11.700 µg/ml.

played an increase in antibody avidity tested with the immunogen MAP[VP1+VP3], probably reflecting the additive effect of specific antibodies mounted against VP1 and VP3 besides antibodies recognising the conformational epitope of MAP[VP1+VP3]. Thus, the affinity constant, calculated by the ELISA, was up to one order of magnitude greater in the sera of the rabbit immunised with MAP entrapped in liposomes than in the rabbit immunised with the same peptide with the classical Freund's adjuvant protocol. Fig. 4 shows an experimental ELISA curve for purified IgG at different MAP[VP1+VP3] coating concentrations.

For the biosensor technology, we chose the strategy of binding the peptide MAP[VP1+VP3] to the chip and utilising the polyclonal IgG as analyte to avoid variability on the coating IgG to the chip.

Kinetic analysis entailed data of a single flow cell after subtraction of the background sensorgram readings. Using the BIAevaluation 3.0.2 software (Biosensor AB), we proceeded to fit data results to three different models predetermined in the BIAevaluation software. The Langmuir model is the simplest model for 1:1 interaction between an analyte (IgG) and immobilised ligand (MAP peptide). The bivalent analyte model assumes that a bivalent analyte (IgG) can

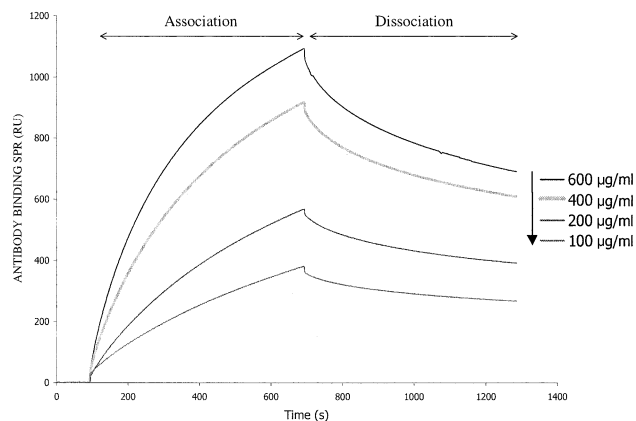


Fig. 5. Typical Biacore sensorgram obtained with different IgG concentrations of immune rabbit anti-MAP[VP1+VP3] that was immobilised on the dextran matrix. Sensorgrams depicting real-time binding interaction between twofold dilutions of immune rabbit IgG interacting at 10  $\mu\text{l}/\text{min}$  with MAP[VP1+VP3] covalently linked to biosensor chip CM5. The antibody association phase is shown for time 140–690 s and is followed immediately by the dissociation phase 690–1300 s. Determination of dissociation rate constants  $K_d$  ( $\text{s}^{-1}$ ) were obtained from each curve as described in Section 2.

bind to one or two ligands or sites in one complexed MAP. The heterogeneous ligand-parallel reaction describes an interaction between one analyte and two independent ligands. This model was selected considering the heterogeneous immobilisation of ligand (amine coupling, the ligand has multiple attachment points) and the nature of the MAP peptide [VP1 and VP3]. In this model, the binding curve obtained is simply the sum of the two independent reactions.

For good fitting to ideal data,  $\chi^2$  may be of the same order of magnitude as the noise in RU; typically less than 2, but in practice, values less than 10 are acceptable. As shown in Table 4, the  $\chi^2$  values of our experimental data do not fit any of the three models. Furthermore, linear transformation of the binding data showed non-linear plots, indicating that the binding follows complex models (data not shown).

Another parameter useful to estimate the affinity is the calculation of the association ( $K_a$ ) and dissociation ( $K_d$ ) constants. The dissociation rate analysis calculates the amount of antibody per second dissociated after reaching the steady state (Fig. 5) and seems to be more discriminative than the  $K_a$  [21,22].

Two different IgG concentrations (400  $\mu\text{g}/\text{ml}$  and 200  $\mu\text{g}/\text{ml}$ ) were used in order to ensure that measurements were

made at the saturation concentration of antibody, conditions in which this kinetic parameter is independent of the IgG concentration. At either concentration, the MAP[VP1+VP3] peptides in liposomes elicit antisera with highest avidity, measured by a reciprocal rate constant ( $1/K_d$ ) of 262 000 which were up to two orders of magnitude greater than observed with the avidity antisera elicited by immunisation with Freund's adjuvant,  $1/K_d$  of 2020 (Table 3).

#### 4. Discussion

The main aim in the development of a peptide-based vaccine is to induce the same immunity as with the whole viral proteins but using selected short peptide fragments containing the most potent antigenic determinants. The methods available for the location of these antigenic determinants can be divided into two groups, experimental and computational. Computational methods are usually based on physicochemical structural properties such as hydrophilicity, surface accessibility and segmental mobility. These data were considered, as previously described, to select VP1 and VP3 peptide fragments containing potentially active B and T cell epitopes [3,23].

Although the most widely used vehicle for vaccine delivery in humans consists of aluminium hydroxide, other vaccine vehicles that have shown promise are liposomes [24]. In our studies, a liposomal formulation containing MAP[VP1+VP3] has proved to be successful in terms of high level of mean antibody content and low reactogenicity.

A way to overcome the loss of non-entrapped peptide during liposome preparation can be the incorporation of hydrophobic anchors to the amino- or carboxy-terminal ends, which on the basis of previous findings dramatically enhances their immunogenicity in the absence of adjuvant [25,26]. Thus, the regioselective  $N^{\epsilon}$ -palmitoyl derivatisation was designed to modify the hydrophobicity of the MAP and to favour the incorporation into the liposome surface.

The rationale for anchoring the palmitoyl-MAP[VP1+VP3] on liposomes was to mimic the external appearance of the virion, particularly of the surface protein. Furthermore, the lipid anchor serves a dual role, as a built-in adjuvant and as a lipid-anchoring moiety [27]. At the same time the combination of adjuvant effects of liposomes and the built-in lipid anchor may replace the need for an extraneous adjuvant such as Freund's, which is toxic and unacceptable for use in humans.

There is general agreement that both encapsulated and surface-bound liposomal antigens can participate in the immune process [28]. In our case, as the peptide construct bears a lipid

Table 4  
Kinetic analysis of the sequential IgG antibody to HAV-MAP[VP1+VP3] peptide by three predefined models (Langmuir, bivalent and heterogeneous ligand)

Weeks	Langmuir		Bivalent		Heterogeneous ligand		
	$K_a$	$\chi^2$	$K_a$	$\chi^2$	$K_{a1}$	$K_{a2}$	$\chi^2$
Rabbit 1							
3	$1.73 \times 10^6$	169	$3.16 \times 10^5$	203	$8.22 \times 10^5$	$1.68 \times 10^{11}$	118
6	$8.27 \times 10^5$	55.9	$4.20 \times 10^4$	47.2	$1.04 \times 10^4$	$1.42 \times 10^9$	22.4
9	$6.38 \times 10^6$	36.5	$6.84 \times 10^3$	31	$6.45 \times 10^6$	$6.49 \times 10^6$	37
12	$8.83 \times 10^5$	142	$1.42 \times 10^4$	144	$3.26 \times 10^6$	$3.25 \times 10^6$	144
Rabbit 2							
3	$1.77 \times 10^6$	105	$2.07 \times 10^5$	4440	$1.95 \times 10^6$	$3.29 \times 10^5$	104
6	$1.52 \times 10^6$	10.4	$3.86 \times 10^5$	9.38	$3.71 \times 10^9$	$6.76 \times 10^5$	1.17
9	$2.17 \times 10^6$	12.2	$2.48 \times 10^5$	12.2	$2.73 \times 10^6$	$1.48 \times 10^6$	12.2
12	$4.24 \times 10^6$	80.5	$1.41 \times 10^5$	79.1	$3.55 \times 10^6$	$4.88 \times 10^6$	80.5

tail of palmitic acid, and liposomes have been prepared by mixing all components, it is logical to assume that the peptide sequence is at least partly integrated between the lipid bilayers of MLV liposomes, thus mimicking the natural presentation of an epitope in the context of an *in vivo* antigenic situation.

Thus, it was gratifying to observe that in rabbit 2 immunisation with MAP[VP1+VP3] in liposomes elicited specific IgG not only against MAP itself but also against the VP3 and VP1 antigens, which are contained in the MAP. However, in rabbit 1, no recognition was observed for the VP3 peptide. This result could be explained by differences in the VP3 conformation presented either in MAP–liposomes or mixed with Freund's adjuvant. Thus, the B cell epitope present in the liposomal preparation appeared to be more accessible to antibodies. Another possibility to explain differences in mounting an immune response is the timing of presentation of the peptide by liposomes in comparison with Freund's adjuvant, and by activating different events in the antigen-presenting cells [29].

Moreover, several factors could contribute to the procedure adopted for serum analysis [30]. First, branched peptides bind more readily to the microtitre wells than do monomeric peptides. Second, multivalent binding between antibody and branched peptide would result in a considerable increase in stability, compared to simple monovalent binding of monomeric peptide. Third, to be immunoreactive monomeric peptides have to both bind to the plastic well and remain available for binding to the antibody, whereas one or more arms of a branched peptide could bind to the plastic and leave the other(s) free to bind to the antibody. It is possible that in binding to the plastic, physical constraints are imposed on a monomeric peptide to prevent it from interacting freely with the antibody.

Antibody affinity constants have been measured by many methods including competitive radioimmunoassay [31], competitive ELISA [32], quantitation of eluted antibody [33], indirect ELISA [19], and more recently SPR technology [34]. These approaches have been applied to measure affinity of monoclonal antibodies but few studies have reported the avidity of polyclonal antibodies that is the physiological immune response after vaccination. We have used two different approaches, an indirect ELISA and a biosensor technology, to estimate the avidity of antibody response to MAP peptides inoculated with the Freund's adjuvant protocol or entrapped in liposomes.

In our studies, the experimental curves to calculate avidity from the ELISA experiment do not fulfil the theoretical curves assumed in Beatty's model, designed for monoclonal antibodies. These discrepancies found in experimental results could be attributed to the complexity of both antigen and antibody analytes. The antigen is a complex peptide, exposing at least three immunoreactive sites, VP1, VP3 and the conformational MAP[VP1+VP3], and the antibody could be reactive with mono- or bivalence.

Rabbit 1 recognised mainly the conformational epitopes of MAP[VP1+VP3] (Fig. 3A) in all serum samples but in bleeds corresponding to weeks 3 and 6 a reactivity against VP1 was also detected. The measure of avidity,  $K_a$ , at these points reaching  $7.3 \times 10^6$  and  $7.05 \times 10^6 \text{ M}^{-1}$  respectively (Table 3), could represent the summatory effect of antibodies reacting with both immunopeptides.

However, in rabbit 2, the calculated avidity increased

throughout the study duration, as the reactivity against MAP[VP1+VP3], VP1 and VP3 increased (Fig. 3B). Hence, the calculated avidity may be an estimation of at least three specific antibodies. As shown in Table 3, the avidity constant  $K_a$  ranges from  $4.56 \times 10^6$  up to  $2.90 \times 10^7 \text{ M}^{-1}$ .

The most problematic feature to calculate the avidity of immune IgG by Biacore technology was to find a mathematical approach that conforms to the interaction model. Several studies adopted a 1:1 solution phase affinity model, whilst others have used a 2:1 model or a model of complex interactions.

The ligand MAP[VP1+VP3] contains more than one epitope, as shown by indirect ELISA on immune sera that recognised the construct MAP[VP1+VP3], as well as each of the linear parent peptides (Fig. 3). Furthermore, the IgG can interact with the ligand by one or two Fab domains with each of the exposed epitopes, thus becoming a complex model of interaction. This is probably one of the reasons why none of the simple analytical models of interactions fit with our data (Table 4). However, comparisons of avidity can be established by examining dissociation rate constants, which are inversely proportional to avidity and independent of concentrations under saturating conditions [21]. Thus, although different measurement units were used, a good correlation was observed between the  $1/K_d$  value from SPR and the calculated  $K_a$  from ELISA experiments ( $r=0.72$  for rabbit 1 and  $r=0.99$  for rabbit 2).

Both ELISA and SPR analysis indicated that liposomes induced more avid antisera than immunisation with Freund's adjuvant in this particular formulation.

In conclusion, we have shown that MAP are able to mount an antibody response either inoculated in Freund's adjuvant or entrapped in liposomes. The liposome preparations of the palmitoyl derivative of MAP[VP1+VP3] induced a stronger immune response, measured in terms of avidity and number of epitopes recognised by the inoculated animal. In the light of these results, the MAP constructs are suitable to be used as immunogens mimicking the native protein, and the liposome formulation of the lipophilic MAP offers a valuable strategy for the design of therapeutic vaccines.

*Acknowledgements:* We gratefully acknowledge Dr P. Casas for valuable help on immunisation protocols. M.G. is also indebted to an EMBO exchange grant.

## References

- [1] Tam, J.P. (1988) Proc. Natl. Acad. Sci. USA 85, 5409–5413.
- [2] Nardin, E.H., Oliveira, G.A., Calvo-Calle, J.M. and Nussenzweig, R.S. (1995) Adv. Immunol. 60, 105–149.
- [3] Haro, I., Pinto, R.M., González-Dankaart, J.F., Pérez, J.A., Reig, F. and Bosch, A. (1995) Microbiol. Immunol. 39, 485–490.
- [4] Bosch, A., González-Dankaart, J.F., Haro, I., Gajardo, R., Pérez, J.A. and Pinto, R.M. (1998) J. Med. Virol. 54, 95–102.
- [5] Pinto, R.M., González-Dankaart, J.F., Sánchez, G., Guix, S., Gómara, M.J., García, M., Haro, I. and Bosch, A. (1998) FEBS Lett. 438, 106–110.
- [6] Firsova, T.V., Pérez, J.A., Reig, F., Kruglov, I.V. and Haro, I. (1996) in: Peptides 1996 (Ramage, R. and Epton, R., Eds.), pp. 383–384, Mayflower Science, UK.
- [7] Gómara, M.J., Riedemann, S., Vega, I., Ibarra, H., Ercilla, G. and Haro, I. (2000) J. Immunol. Methods 234, 23–24.
- [8] Gómara, M.J., Ercilla, G., Alsina, M.A. and Haro, I. (2000) J. Immunol. Methods 246, 13–24.
- [9] Hopp, T.P. (1984) Mol. Immunol. 1, 13–16.

- [10] Uhl, B., Wolf, B., Scwinde, A., Jung, G., Bessler, W.G. and Hauschildt, S. (1991) *J. Leukoc. Biol.* 50, 10–18.
- [11] Wolf, B., Uhl, B., Hauschild, S., Metzger, J. and Bessler, W.G. (1989) *Immunobiology* 180, 93–100.
- [12] Tam, P.J., Clavijo, P., Lu, Y.-A., Nussenzweig, V., Nussenzweig, R. and Zavala, V. (1990) *J. Exp. Med.* 171, 299–306.
- [13] Nardelli, B., Lu, Y.-A., Defoort-Delpierre, C., Shiu, D., Profy, A.T. and Tam, J.P. (1992) *J. Immunol.* 148, 914–920.
- [14] McLean, G., Cross, A., Munns, M. and Marsden, H.S. (1992) *J. Immunol. Methods* 155, 113–120.
- [15] Chan, W.C. and White, P.D. (Eds.) (2000) *Fmoc Solid Phase Peptide Synthesis: A Practical Approach*, Oxford University Press, Oxford.
- [16] Bycroft, B.W., Chan, W.C., Chhabra, S.R. and Hone, N.D. (1993) *J. Chem. Soc. Chem. Commun.* 778–779.
- [17] Garcia, M., Alsina, M.A., Reig, F. and Haro, I. (2000) *Vaccine* 18, 276–283.
- [18] McClare, C.W. (1971) *Anal. Biochem.* 39, 527–530.
- [19] Beatty, J.D., Beatty, B.G. and Vlahos, W.G. (1987) *J. Immunol. Methods* 100, 173–179.
- [20] Steward, M.W. and Steensgaard, J. (1983) *Antibody Affinity: Thermodynamic Aspects and Biological Significance*, CRC Press, Boca Raton, FL.
- [21] Van Cott, T.C., Bethke, F.R., Polonis, V.R., Gorny, M.K., Zolapazner, S., Redfield, R.R. and Birx, D.L. (1994) *J. Immunol.* 153, 449–459.
- [22] Christodoulides, M., Rattue, E. and Heckels, J.E. (2000) *Vaccine* 18, 131–139.
- [23] Garcia, M., Pujol, M., Reig, F., Alsina, M.A. and Haro, I. (1996) *Analyst* 121, 1583–1588.
- [24] Alving, C.R. (1991) *J. Immunol. Methods* 140, 1–13.
- [25] Deprez, B., Sauzet, J.P., Boutillon, C., Martinon, F., Tartar, A., Sergheraert, C., Guillet, J.G., Gomard, E. and Gras-Masse, H. (1996) *Vaccine* 14, 375–382.
- [26] Benmohamed, L., Thomas, A., Bossus, M., Brahimi, K., Wubben, J., Gras-Masse, H. and Druilhe, P. (2000) *Vaccine* 18, 2843–2855.
- [27] Nardelli, B., Defoort, J.P., Huang, W. and Tam, J.P. (1992) *Res. Hum. Retroviruses* 8, 1405–1407.
- [28] Van Rooijen, N. and Su, D. (1989) in: *Immunological Adjuvants and Vaccines* (Gregoriadis, G., Allsion, A.C. and Poste, G., Eds.), p. 95, Plenum Press, New York.
- [29] Steward, M.W. and Lew, A.M. (1985) *J. Immunol. Methods* 78, 173–176.
- [30] Tam, J.P. and Zavala, F. (1989) *J. Immunol. Methods* 124, 53–61.
- [31] Friguet, B., Chaffotte, A.F., Djavadi-Ohanian, L. and Goldberg, M.E. (1985) *J. Immunol. Methods* 77, 305–319.
- [32] Pullen, G.R., Fitzgerald, M.G. and Hosking, C.S. (1986) *J. Immunol. Methods* 86, 83–90.
- [33] Altschuh, D., Dubs, M.C., Weiss, E., Zeder-Lutz, G. and van Regenmortel, M.H.V. (1982) *Biochemistry* 31, 6298–6304.
- [34] Malmqvist, M. (1993) *Nature* 361, 186–187.